

Analysis of Noise Reduction Method for Supersonic Jets in the Sideline and Upstream Directions

Trushant K. Patel and Steven A. E. Miller
trushant@ufl.edu
saem@ufl.edu

Theoretical Fluid Dynamics and Turbulence Group
Department of Mechanical and Aerospace Engineering
University of Florida



December 10, 2020

This work is supported by the Office of Naval Research Grant
N00014-17-1-2583

Any opinions, findings, and conclusions or recommendations expressed in this material are those of the author(s) and do not necessarily reflect the views of the Office of Naval Research

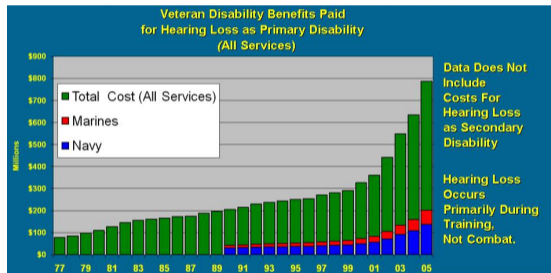
- 1 Motivation
- 2 Identification of Source Terms
- 3 Statistical Prediction Models
- 4 Noise Reduction Technique
- 5 Summary

Motivation

- More than **107,000** sailors are living and working aboard US Navy ships
- Over **a billion dollars** were spent **each year** by US Department of Veterans Affairs for **hearing loss disability** benefits in the last decade¹



US Navy Public Release Photo: 180123-N-GP724-1102

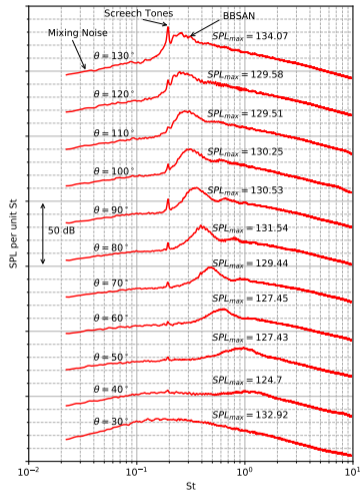
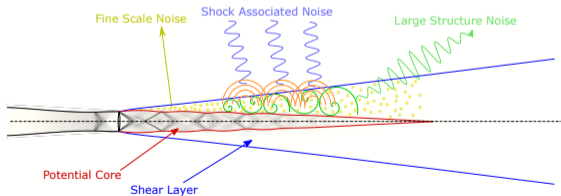


Source: https://www.public.navy.mil/navsafecen/Pages/acquisition/noise_control.aspx

¹Doychak J., "Department of Navy Jet Noise Reduction Project Overview," *15th Annual Partners in Environmental Technical Symposium and Workshop*, Washington D.C., 2010.

Components of Jet Noise

- Two main components of jet noise - turbulent mixing noise and shock-associated noise
- Broadband shock-associated noise is generated due to *coherent interaction* of large-scale structures with the shock-cell structure
- Fine-scale mixing noise is relatively spatially incoherent
- Mainly dominant in the sideline and upstream direction

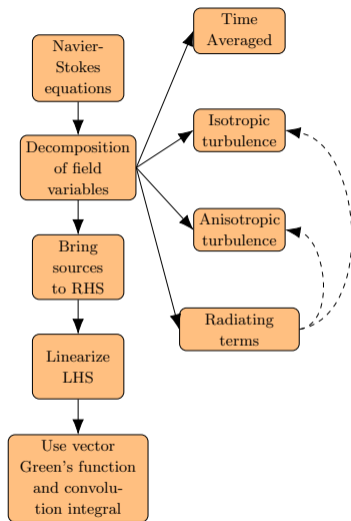


Noise spectra at different observer locations²

²Brown, C., and Bridges, J. E., "Small Hot Jet Acoustic Rig Validation," NASA/TM-2006-214234, 2006.

Prediction Model³

- We start with the Navier-Stokes equations as the governing equations
- The *field-variables* such as density, velocity, pressure, and temperature are decomposed into **base flow** (\bar{q}), **aerodynamic fluctuations** (\check{q} and \hat{q}), and **acoustic fluctuations** (q' and q'')
- The aerodynamic turbulent fluctuations (sources) are brought to the right-hand side
- The radiating acoustic components (propagators) are brought on the left-hand side
- The spectral density of the radiating components is obtained by *convolving* the vector Green's function with the source terms present on the right-hand side



³Miller, S. A. E., "Noise from Isotropic Turbulence," *AIAA Journal*, Vol. 55, No. 3, 2017.

After some simplifications⁴, we obtain the spectral density of the field variable as

$$S_k^\perp(\mathbf{x}, \omega) = \int_{-\infty}^{\infty} \cdots \int_{-\infty}^{\infty} \sum_{m=0}^4 \sum_{n=0}^4 q_{g,k}^{*\perp,m}(\mathbf{x}; \mathbf{y}, \omega) q_{g,k}^{\perp,n}(\mathbf{x}; \mathbf{y} + \boldsymbol{\eta}, \omega) R_{m,n}^\perp(\mathbf{y}, \boldsymbol{\eta}, \tau) e^{i\omega\tau} d\tau d\boldsymbol{\eta} d\mathbf{y},$$

where

$$R_{m,n}^\perp(\mathbf{y}, \boldsymbol{\eta}, \tau) = \langle \Theta_m(\mathbf{y}, \tau) \Theta_n(\mathbf{y} + \boldsymbol{\eta}, \tau + \Delta\tau) \rangle = \int_{-\infty}^{\infty} \Theta_m(\mathbf{y}, \tau) \Theta_n(\mathbf{y} + \boldsymbol{\eta}, \tau + \Delta\tau) d\Delta\tau$$

Substituting $k = 4$ to find the spectral density of pressure, we obtain

$$S_4^\perp(\mathbf{x}, \omega) = \int_{-\infty}^{\infty} \cdots \int_{-\infty}^{\infty} \sum_{m=0}^4 \sum_{n=0}^4 p_g^{*\perp,m}(\mathbf{x}; \mathbf{y}, \omega) p_g^{\perp,n}(\mathbf{x}; \mathbf{y} + \boldsymbol{\eta}, \omega) R_{m,n}^\perp(\mathbf{y}, \boldsymbol{\eta}, \tau) e^{i\omega\tau} d\tau d\boldsymbol{\eta} d\mathbf{y}$$

⁴Patel T. K., and Miller, S. A. E., "Statistical sources for broadband shock-associated noise using the Navier-Stokes equations," *The Journal of the Acoustical Society of America*, Vol. 146, No. 6, 2019.

- The source terms on the RHS are

$$\Theta_0 = -\frac{\partial \underline{p}}{\partial t} - \frac{\partial \underline{\rho} \underline{u}_j}{\partial x_j}$$

$$\Theta_i = -\frac{\partial \underline{\rho} \underline{u}_i}{\partial t} - \frac{\partial \underline{\rho} \underline{u}_i \underline{u}_j}{\partial x_j} - \frac{\partial \underline{p}}{\partial x_j} \delta_{ij} + \frac{\partial}{\partial x_j} \left[\mu \left(\frac{\partial \underline{u}_i}{\partial x_j} + \frac{\partial \underline{u}_j}{\partial x_i} \right) \right] - \frac{2}{3} \frac{\partial}{\partial x_j} \left[\mu \frac{\partial \underline{u}_k}{\partial x_k} \right]$$

$$\Theta_4 = -\frac{\partial \underline{p}}{\partial t} - \frac{\gamma - 1}{2} \frac{\partial \underline{\rho} \underline{u}_k \underline{u}_k}{\partial t} - \gamma \frac{\partial \underline{u}_j \underline{p}}{\partial x_j} - \frac{\gamma - 1}{2} \frac{\partial \underline{\rho} \underline{u}_j \underline{u}_k \underline{u}_k}{\partial x_j} + (\gamma - 1) \frac{\partial}{\partial x_j} \left[\frac{c_p \mu}{Pr} \frac{\partial T}{\partial x_j} \right] \\ + (\gamma - 1) \frac{\partial}{\partial x_j} \left[\mu \underline{u}_i \left(\frac{\partial \underline{u}_i}{\partial x_j} + \frac{\partial \underline{u}_j}{\partial x_i} \right) \right] - \frac{2}{3} \delta_{ij} \frac{\partial}{\partial x_j} \left[\mu \underline{u}_i \frac{\partial \underline{u}_k}{\partial x_k} \right]$$

- Different researchers^{5,6} have found that viscous terms are not important for sound generation

⁵Lighthill, M. J., "On Sound Generated Aerodynamically I. General Theory," *Proceedings of the Royal Society of London. Series A. Mathematical, Physical, and Engineering Sciences*, Vol. 211, No. 1107, 1952.

⁶Mollö-Christensen, E., "Jet Noise and Shear Flow Instability Seen From an Experimenter's Viewpoint," *Journal of Applied Mechanics*, Vol. 34, No. 1, 1967.

- The same FSMN source term proposed by Tam and Auriault⁷ is also obtained from the Navier-Stokes equations as

$$R_{\text{FSMN}} = (\gamma - 1)^2 \left\langle \frac{D\bar{\rho}^{(1)} K_s^{(1)}}{D\tau}, \frac{D\bar{\rho}^{(2)} K_s^{(2)}}{D\tau} \right\rangle \approx (\gamma - 1)^2 \frac{\bar{\rho}^2 K_s^2}{\tau_s^2} \check{R}$$

- The only term that scales as β^4 for BBSAN is the product of gradient of mean pressure and the large-scale velocity fluctuations

$$R_{\text{BBSAN}} = \gamma^2 \left\langle \frac{\partial \underline{u}_j^{(1)} \underline{p}^{(1)}}{\partial y_j}, \frac{\partial \underline{u}_m^{(2)} \underline{p}^{(2)}}{\partial y_m} \right\rangle \approx \gamma^2 \frac{\partial \bar{p}^{(1)}}{\partial y_j} \frac{\partial \bar{p}^{(2)}}{\partial y_m} \hat{u}_j^{(1)} \hat{u}_m^{(2)} \hat{R}$$

⁷Tam, C. K. W., and Auriault, L., "Jet Mixing Noise from Fine-Scale Turbulence," AIAA Journal, Vol. 37, No. 2, 1999.

For fine-scale noise, we use the same normalized two-point cross-correlation as Tam and Auriault as

$$\check{R} = \exp\left(-\frac{|\xi|}{\bar{u}\tau_s} - \frac{\ln 2}{l_s^2} [(\xi - \bar{u}\tau)^2 + \eta^2 + \zeta^2]\right)$$

We obtain the spectral density as

$$S_4^\perp(\mathbf{x}, \omega) = \left(\frac{\pi}{4 \ln 2}\right)^{3/2} (\gamma - 1)^2 \iiint_{-\infty}^{\infty} \frac{\bar{\rho}^2 K_s^2 l_s^3}{\tau_s} |p_g^{\perp 4}(\mathbf{x}, \mathbf{y}, \omega)|^2 \frac{\exp\left[-\frac{\omega^2 l_s^2}{\bar{u}^2 (4 \ln 2)}\right]}{\left[1 + \left(1 - \frac{\bar{u}}{c_\infty} \cos \theta\right)^2 \omega^2 \tau_s^2\right]} d\mathbf{y}$$

The resulting model is equivalent to the Tam and Auriault model

We now consider different length scales in the cross-stream directions and model the normalized two-point cross-correlation as

$$\hat{R} = \exp\left[-\frac{|\tau|}{\tau_s}\right] \exp\left[-\frac{(\xi - \mathbf{u}_c \tau)^2}{l_1^2}\right] \exp\left[-\frac{\eta^2}{l_2^2} - \frac{\zeta^2}{l_3^2}\right]$$

After integrating and simplifying, we obtain a closed-form prediction model as

$$S_4^\perp(\mathbf{x}, \omega) = \frac{\gamma^2 \omega^2}{16\pi\sqrt{\pi}c_\infty^4 r^2} \iint_{-\infty}^{\infty} l_1 l_2 l_3 \tau_s \exp\left[-\frac{\omega^2}{4a_\infty^2} \sin^2 \theta (l_2^2 \cos^2 \phi + l_3^2 \sin^2 \phi)\right] \frac{\partial \bar{p}}{\partial y_j}(\mathbf{y}) \hat{u}_j(\mathbf{y})$$

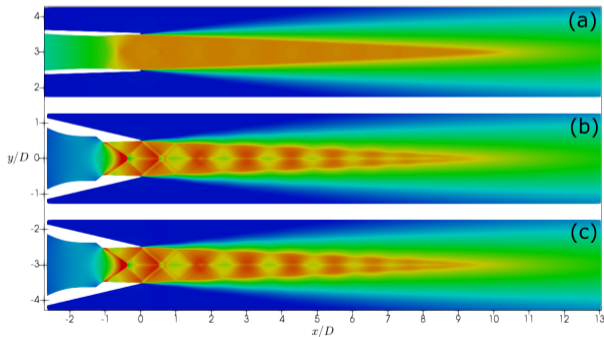
$$\left[\int_{-\infty}^{\infty} \frac{\exp\left[-l_1^2 \left(\kappa - \frac{\omega \cos \theta}{c_\infty}\right)^2 / 4\right]}{\left[1 + \left(1 - M_c \cos \theta + \frac{\mathbf{u}_c \kappa}{\omega}\right)^2 \omega^2 \tau_s^2\right]} \frac{\partial \bar{p}}{\partial y_m}(\kappa, y_2, y_3) d\kappa \right] \hat{u}_m(\mathbf{y}) d\mathbf{y},$$

However, very good prediction results are obtained using LES data with the identified source term and free-space Green's function⁸

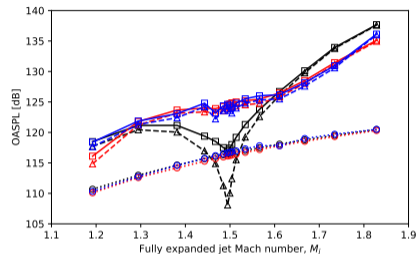
⁸Shen, W., Patel, T. K., and Miller, S. A. E., "Extraction of Large-Scale Coherent Structures from Large Eddy Simulation of Supersonic Jets for Shock-Associated Noise," *AIAA SciTech 2020 Forum*, AIAA Paper No. 2020-0742, 2020.

Comparison of Different Nozzle Geometries

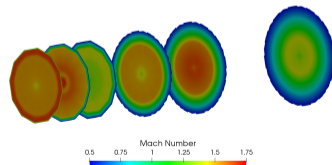
- The biconic and faceted nozzle contains shocks even at design conditions
- Hence, shock-associated noise is present even at design condition



(a) SMC016 nozzle (b) biconic nozzle (c) faceted nozzle

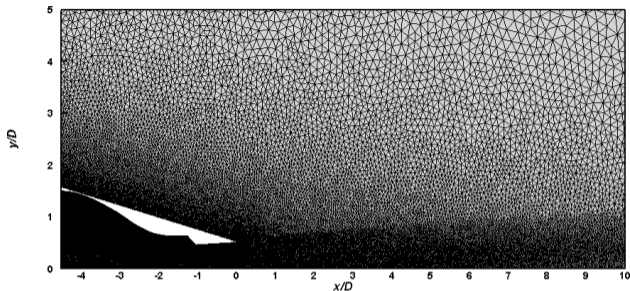


◯ FSMN - SMC016 ◯ FSMN - Biconic ◯ FSMN - Faceted
 △ BBSAN - SMC016 △ BBSAN - Biconic △ BBSAN - Faceted
 □ Combined - SMC016 □ Combined - Biconic □ Combined - Faceted

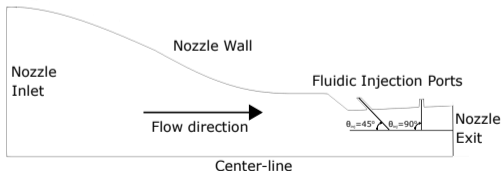


Nozzle Design and Computational Grid

- The design of the fluidic injection ports is performed following Morris et al.⁹
- $D_{inj} = 0.05D$; $m_{ratio} = 2.41\%$
- Fluidic injection ports are located at 20% and 70% of the divergent section with 45° and 90° injection angles

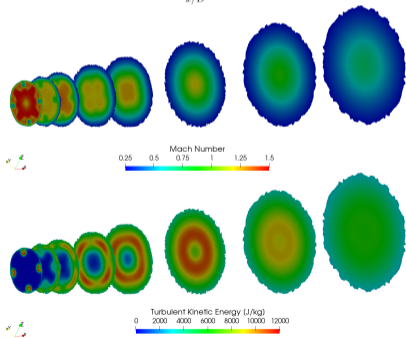
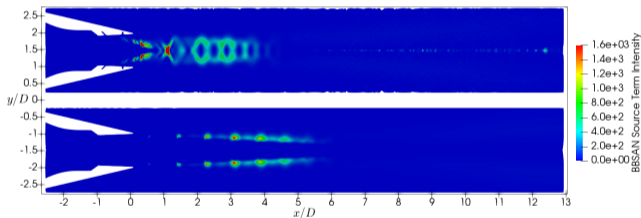
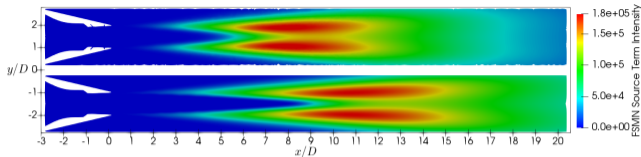
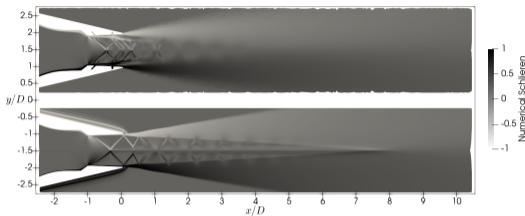


Nozzle		Injector	
NPR	TTR	IPR	ITR
2.750	3.000	2.750	1.000
3.100	3.000	3.100	1.000
3.670	3.000	3.670	1.000
4.320	3.000	4.320	1.000
5.200	3.000	5.200	1.000



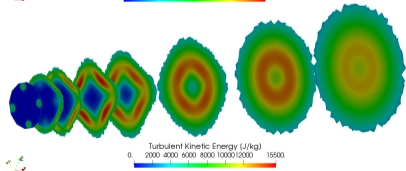
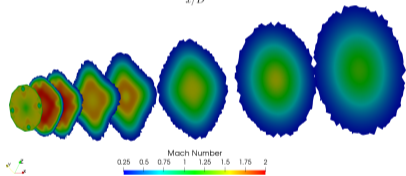
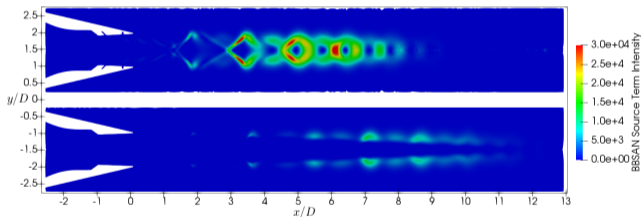
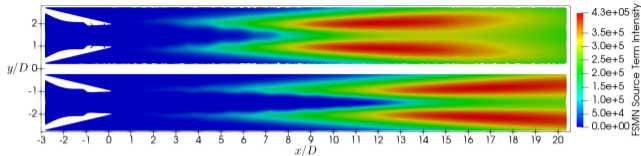
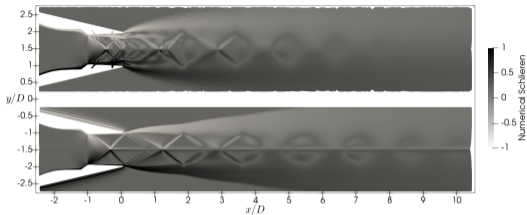
⁹Morris, P. J., et al., "Noise Reduction in Supersonic Jets by Nozzle Fluidic Inserts," *Journal of Sound and Vibration*, Vol. 332, No. 17, 2013.

Results for NPR = 2.750 and TTR = 3.00



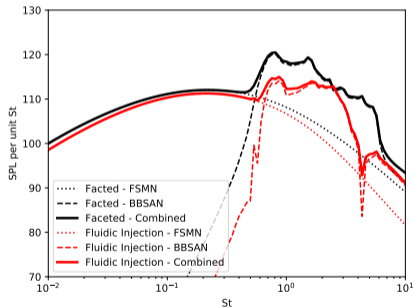
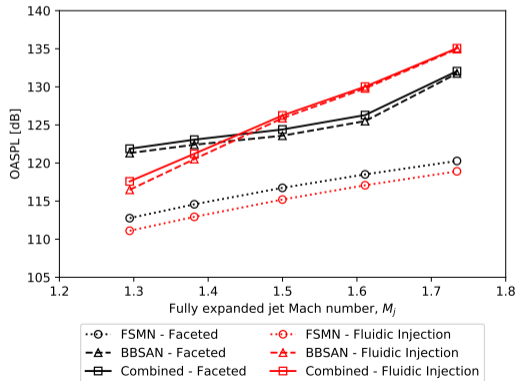
Clockwise starting from the top-left: Numerical schlieren comparison, FSMN source location comparison, BBSAN source location comparison of the fluidic insert nozzle with the faceted nozzle, and Mach no. and TKE contours at different cross-sections

Results for NPR = 5.200 and TTR = 3.00



Clockwise starting from the top-left: Numerical schlieren comparison, FSMN source location comparison, BBSAN source location comparison of the fluidic insert nozzle with the faceted nozzle, and Mach no. and TKE contours at different cross-sections

- BBSAN reduces at over-expanded condition and increases at under-expanded conditions
- BBSAN OASPL reduces by 6 dB at $NPR = 2.750$ and increases by 4 dB at $NPR = 5.200$
- FSMN OASPL reduces by 1.75 dB at all operating conditions



- Identified the FSMN and BBSAN source term from the Navier-Stokes equations
- Developed statistical models for FSMN and BBSAN
- Noise radiating from different nozzle geometries were compared using the identified source term
- Fluidic injection noise reduction technique was analysed using the identified source terms
- Approximately similar noise reduction is obtained in the present work when compared to the experiments of Morris et al.¹⁰
- The identified source terms can be used for quantifying noise reduction due to different noise reduction techniques in the future

¹⁰Morris, P. J., McLaughlin, D. K., and Kuo, C.-W., "Noise Reduction in Supersonic Jets by Nozzle Fluidic Inserts," *Journal of Sound and Vibration*, Vol. 332, No. 17, 2013.

Thank You for your Attention!
Questions?